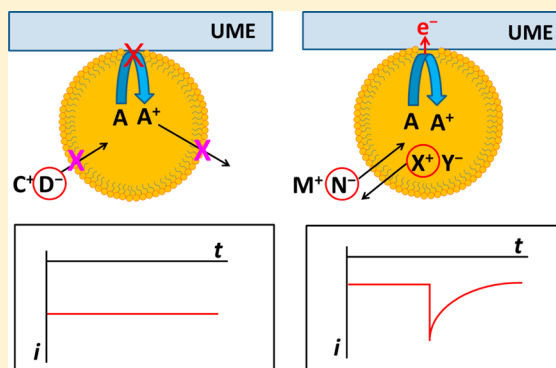


## Probing Ion Transfer across Liquid–Liquid Interfaces by Monitoring Collisions of Single Femtoliter Oil Droplets on Ultramicroelectrodes

Haiqiang Deng,<sup>†,‡</sup> Jeffrey E. Dick,<sup>†,‡</sup> Sina Kummer,<sup>§</sup> Udo Kragl,<sup>§</sup> Steven H. Strauss,<sup>||</sup> and Allen J. Bard<sup>\*,†</sup><sup>†</sup>Center for Electrochemistry, Department of Chemistry, The University of Texas at Austin, Austin, Texas 78712, United States<sup>§</sup>Division of Analytical and Technical Chemistry, Institute of Chemistry, University of Rostock, D-18059 Rostock, Germany<sup>||</sup>Department of Chemistry, Colorado State University, Fort Collins, Colorado 80523, United States

## Supporting Information

**ABSTRACT:** We describe a method of observing collisions of single femtoliter (fL) oil (i.e., toluene) droplets that are dispersed in water on an ultramicroelectrode (UME) to probe the ion transfer across the oil/water interface. The oil-in-water emulsion was stabilized by an ionic liquid, in which the oil droplet trapped a highly hydrophobic redox probe, rubrene. The ionic liquid also functions as the supporting electrolyte in toluene. When the potential of the UME was biased such that rubrene oxidation would be possible when a droplet collided with the electrode, no current spikes were observed. This implies that the rubrene radical cation is not hydrophilic enough to transfer into the aqueous phase. We show that current spikes are observed when tetrabutylammonium trifluoromethanesulfonate or tetrahexylammonium hexafluorophosphate are introduced into the toluene phase and when tetrabutylammonium perchlorate is introduced into the water phase, implying that the ion transfer facilitates electron transfer in the droplet collisions. The current ( $i$ )–time ( $t$ ) behavior was evaluated quantitatively, which indicated the ion transfer is fast and reversible. Furthermore, the size of these emulsion droplets can also be calculated from the electrochemical collision. We further investigated the potential dependence on the electrochemical collision response in the presence of tetrabutylammonium trifluoromethanesulfonate in toluene to obtain the formal ion transfer potential of tetrabutylammonium across the toluene/water interface, which was determined to be 0.754 V in the inner potential scale. The results yield new physical insights into the charge balance mechanism in emulsion droplet collisions and indicate that the electrochemical collision technique can be used to probe formal ion transfer potentials between water and solvents with very low ( $\epsilon < 5$ ) dielectric constants.



I on transfer (IT) across the interface between two immiscible electrolyte solutions (ITIES) has been extensively investigated. ITIES studies involve ion transfer across water and a relatively polar organic solvent, for example, 1,2-dichloroethane (DCE, dielectric constant  $\epsilon = 10.42$ )<sup>1</sup> or nitrobenzene (NB,  $\epsilon = 35.6$ )<sup>2</sup> to form the interface that can be polarized.<sup>3</sup> Generally, a four-electrode setup<sup>4–6</sup> and liquid-modified three-electrode system<sup>7–10</sup> for macro-ITIES, supported micro- and nano-ITIES,<sup>11</sup> and scanning electrochemical microscopy (SECM)<sup>12,13</sup> are used in externally polarizing the ITIES to facilitate ion transfer. A small amount of literature exists on ITIES electrochemistry employing organic solvents with low dielectric constants, for example, toluene ( $\epsilon = 2.38$ ),<sup>14,15</sup> because the high resistance of low dielectric media makes the electrochemistry and ITIES studies of various analytes of interest difficult to investigate. Therefore, developing relevant techniques could set the foundation for studying electrochemistry and ITIES in low dielectric constant media.<sup>16</sup>

Recently, we developed a methodology to study electrochemistry in low dielectric constant media by trapping an electrically neutral, hydrophobic redox molecule into a stable

femtoliter (fL) oil droplet.<sup>17–20</sup> When the emulsion droplet collides with an ultramicroelectrode (UME) surface, the contents of the droplet are electrolyzed at the electrode that is biased at a potential where the trapped redox species can be oxidized or reduced in the oil phase. This method of analyzing fL droplet reactors is termed the emulsion droplet reactor (EDR) method. The ionic liquid trihexyltetradecylphosphonium bis(trifluoromethylsulfonyl)amide (IL-PA) was used as both the supporting electrolyte in the oil phase and the emulsifier, stabilizing emulsion droplets. A single collision of an oil droplet is observed as an exponential blip-type current ( $i$ ) transient as a function of time ( $t$ ). Relevant information, including size distribution and concentration of the emulsion oil droplets, can be obtained via analysis of the  $i$ – $t$  profile.<sup>17,19,20</sup> To maintain charge neutrality in the oil phase during the Faradaic process, either the generated (oxidized or reduced) charged redox species in the oil droplet must enter

Received: May 3, 2016

Accepted: July 7, 2016

Published: July 7, 2016

the aqueous continuous phase or ion transfer across the ITIES must occur to facilitate electron transfer (ET).

We show that collisions of toluene droplets filled with rubrene and IL-PA are only electrochemically observed when other ions (existing in either the oil phase or aqueous phase) are transferred through the ITIES. These ions facilitate electron transfer of rubrene at the UME surface, implying that the rubrene radical cation is too hydrophobic to enter the water. Different ions, capable of transferring across the ITIES both to and from the oil droplet, were investigated to confirm the hypothesis that the oxidation of rubrene in the toluene/IL-PA droplets required the transfer of ions. A voltammogram built from electrochemical collisions at different potentials was compared to the cyclic voltammogram (CV) in the bulk of oil phase to estimate the formal ion transfer potential (vide infra). We also present that other hydrophobic molecules (rather than rubrene) will show a collision signal without other ions to facilitate their electron transfer, implying that the charged species generated during the collision at the electrode are able to enter the water phase to maintain charge neutrality. The proposed methodology allows for the study of electron transfer facilitated by ion transfer across an ITIES. The method also allows for measurements in low dielectric constant media.

## EXPERIMENTAL SECTION

**Reagents and Materials.** All reagents were used as received without further purification unless otherwise mentioned. Rubrene (R,  $\geq 98\%$ , Figure S1A in Supporting Information), ferrocene (Fc, 98%), decamethylferrocene (DMFc, 97%, Figure S1B), ferrocenylmethanol (FcMeOH, 97%), sodium tetrphenylborate (NaTPB,  $\geq 99.5\%$ ), tetrabutylammonium trifluoromethanesulfonate (TBAOTf,  $\geq 99.5\%$ ), tetrahexylammonium hexafluorophosphate (THAPF<sub>6</sub>,  $\geq 97\%$ ), trihexyltetradecylphosphonium bis(trifluoromethylsulfonyl)amide (IL-PA,  $\geq 95\%$ ), toluene (99.9%), and concentrated sulfuric acid (95–98%) were obtained from Sigma-Aldrich. Sodium hydroxide monohydrate (NaOH·H<sub>2</sub>O,  $\geq 99.9995\%$ ), tetrabutylammonium perchlorate (TBAClO<sub>4</sub>, 99%), and potassium nitrate (KNO<sub>3</sub>) were purchased from Fluka, ACROS, and Fisher Scientific, respectively. The compound 1,1',3,3'-tetra(2-methyl-2-nonyl)ferrocene (DEC, Figure S1C) was synthesized as described elsewhere.<sup>21</sup> Pt (99.99%, 10 or 25  $\mu\text{m}$  in diameter) wire was obtained from Goodfellow (Devon, PA). All the aqueous solutions were prepared from the Millipore water ( $\geq 18.2 \text{ M}\Omega\text{-cm}$ ).

**Instrumentation.** All voltammetric measurements were performed using a CHI model 900 or 900B potentiostat (CH Instruments, Austin, Texas) with a one-compartment three-electrode glass cell housed in a Faraday cage. A Pt wire was used as the counter electrode, with an Ag/AgCl/1 M KCl reference electrode or an Ag wire quasi-reference electrode, respectively. The working electrode, Pt UME, was prepared according to the methodology described elsewhere.<sup>22</sup> Prior to each electrochemical measurement, the Pt UME was cycled between  $-0.215$  and  $1 \text{ V}$  versus Ag/AgCl/1 M KCl (0.1 V/s) in 0.5 M H<sub>2</sub>SO<sub>4</sub> under argon until a clear and stable hydrogen-under-potential-deposition feature was achieved. A Q500 ultrasonic processor (Qsonica, Newtown, CT) with a microtip probe was employed to create the emulsions. The dynamic light scattering (DLS) experiments were carried out using a Zetasizer Nano ZS instrument (Malvern, Westborough, MA).

**Preparation of the Emulsions.** The toluene o/w emulsion was prepared first by dissolving rubrene (5 mM) and IL-PA

(400 mM) in toluene, followed by mixing 0.1 mL of toluene (rubrene + IL-PA) with 5 mL of Millipore water in a glass vial. The resulting mixture was then vortexed vigorously for 20 s, and an ultrasonic power (500 W, amplitude 40%) was applied immediately using the pulse mode (7 s on, 3 s off, 26 cycles repeated). The as-prepared emulsion was stable for several hours and shown in Figure S2A. The average diameter of the toluene (rubrene + IL-PA)/water emulsion droplets was 894 nm measured by DLS. The number of the toluene (rubrene) emulsion droplets was calculated approximately by the total toluene volume (0.1 mL) divided by the average emulsion droplet volume (0.37 fL, assumed to be a sphere with diameter in 894 nm). Accordingly, the molar concentration of the emulsion droplets was obtained to be 87.12  $\mu\text{M}$  and afterward diluted 26 $\times$  (3.35  $\mu\text{M}$ ) for the collision measurements. For investigating the cation transfer or anion transfer across the o/w interface using rubrene as the redox probe, a variety of salts were dissolved in either the toluene phase or the aqueous phase, respectively. The details have been summarized in Table S1. Note that all the experiments using rubrene as the redox probe were carried out in the dark to avoid possible photo-oxidation of rubrene.<sup>23</sup> The toluene (DMFc + IL-PA)/water emulsion and toluene (DEC + IL-PA)/water emulsion were prepared as above, except a different redox probe in a different concentration was employed. The electrochemical collision experiment was normally completed within 1 h.

## RESULTS AND DISCUSSION

**Overview.** The overall reaction during the single emulsion droplet collision electrochemistry is an electron transfer coupled with ion transfer, schematically described in Figure 1C and eqs 1 (cation X<sup>+</sup> transfer driven by A oxidation) and 2

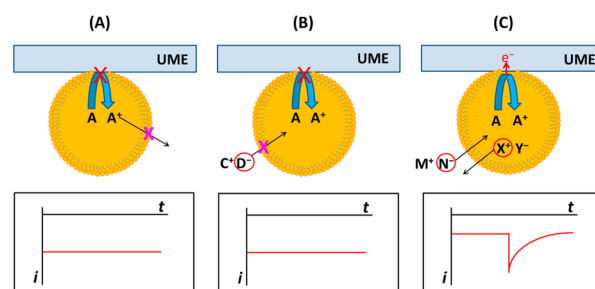
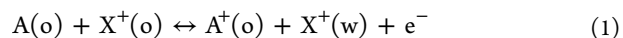


**Figure 1.** Schematic description of the electrochemistry of the single emulsion droplet collision on the UME, in which a hydrophobic redox probe, A, is trapped in the oil phase (in yellow). Tadpole-shaped molecules surrounding the perimeter of the oil droplet represent IL-PA molecules. (A, B) Only a residual background current is observed when either the oxidized product of A, A<sup>+</sup>, cannot leave the oil droplet or a hydrophilic anion, D<sup>-</sup>, cannot enter the droplet. (C) Upon oxidation of A to A<sup>+</sup> at its diffusion-limited oxidation potential, X<sup>+</sup> leaves or N<sup>-</sup> enters the droplet to maintain the charge balance, resulting in the electrolysis of A in the droplet.

(anion N<sup>-</sup> transfer driven by A oxidation). Here “o” represents the oil phase (toluene in this case) and “w” stands for the aqueous phase. In Figure 1A,B, only a residual background current without current spikes is observed if either A<sup>+</sup> (oxidized product of A) cannot leave the oil droplet or aqueous, hydrophilic anion D<sup>-</sup> cannot get into the droplet, respectively.





**Electrochemical Properties of Rubrene in Toluene Solution.** To compare the same reaction within an emulsion droplet in collision experiments, cyclic voltammetry on a 10  $\mu\text{m}$  Pt UME in 5 mM rubrene in bulk toluene solution with 400 mM IL-PA was recorded and is shown in Figure 2A. The

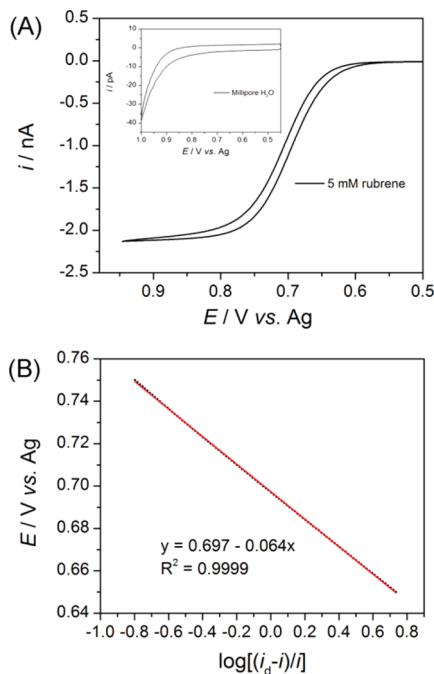


**Figure 2.** (A) CV of freshly prepared 5 mM rubrene and 400 mM IL-PA in toluene on a Pt UME (diameter = 10  $\mu\text{m}$ ) at a scan rate of 10  $\text{mV s}^{-1}$ . The potential scale was referred to the Ag quasi-reference electrode. The inset shows the oxidative potential window (10  $\text{mV s}^{-1}$ ) for the Millipore water on the same Pt UME vs. Ag for comparison. (B) Black dots represent the dependence of the applied electrode potential from 0.65 to 0.75 V on the logarithm of  $(i_d - i)/i$  for the forward scan of rubrene oxidation in (A), where  $i_d$  represents the diffusion-limited current at 0.946 V and  $i$  is the current at the specific potential. The red solid line is the best linear fit curve with a correlation coefficient of  $R^2 = 0.9999$ .

voltammogram shows a sigmoidal wave for the one-electron oxidation of rubrene with a low capacitive current. Rubrene oxidation starts at approximate 0.6 V versus a silver quasi-reference electrode and reaches a steady-state value at 0.85 V. Inset in Figure 2A shows the oxidative potential window for the Millipore water on Pt UME versus Ag, indicating 0.9 V is the highest potential that can be applied in the emulsion droplet collision experiments. Furthermore, it can be seen from Figure 2B that the linear relationship between the applied electrode potential  $E$  and  $\log[(i_d - i)/i]$  has a slope of  $-64 \text{ mV}$ , which is near the theoretical value of  $-59 \text{ mV}$ ,<sup>24</sup> implying rubrene oxidation at the Pt UME surface is Nernstian and the uncompensated solution  $iR$  drop in toluene is negligible. Furthermore, from the intercept on the  $E$  axis of the best fit curve for  $E$  versus  $\log[(i_d - i)/i]$  in Figure 2B, the half-wave potential  $E_{1/2}$  and hence the formal potential  $E^{0'}$  (0.697 V) for  $R^{*+}/R$  was obtained. The diffusion coefficient of R in toluene (400 mM IL-PA) was calculated by eq SIS to be  $2.21 \times 10^{-6} \text{ cm}^2 \text{ s}^{-1}$ .

**Collision Experiments of the Toluene (Rubrene + IL-PA)/Water Emulsion Droplets. Effect of Ions on Amperometric Response.** The collision experiments employing the toluene (rubrene + IL-PA)/water emulsions with and without additional ions in the oil or aqueous phases are summarized in Table S1 and shown in Figure 3. Figure 3A (black line) shows that without additional ions in both toluene and water phases, no current spikes are observed during the collision experiments. It also implies that the impurities in the commercial IL-PA do not have an observable effect on the experimental results. Charge neutrality in the oil droplet can be achieved under three

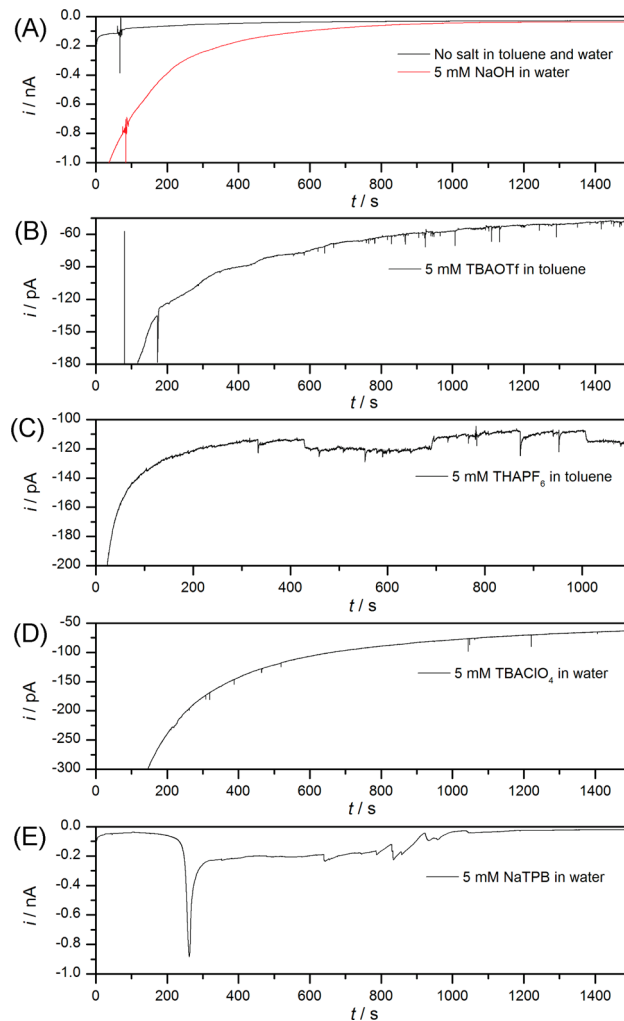


**Figure 3.** (A) Amperometric  $i-t$  curve of collisions of the toluene emulsion droplets (5 mM rubrene + 400 mM IL-PA) in 3.35 pM on the Pt UME biased at 0.9 V vs. Ag wire. The black curve represents the case of no additional salts in both toluene and aqueous phases, while the red curve obtained with the identical emulsion in 5 mM NaOH in the continuous aqueous phase. (B, C) Amperometric  $i-t$  curves of collisions of the toluene emulsion droplets (5 mM rubrene + 5 mM TBAOTf + 400 mM IL-PA, (B)); 5 mM rubrene + 5 mM THAPF<sub>6</sub> + 400 mM IL-PA, (C)) in 3.35 pM on the Pt UME biased at 0.9 V vs. Ag wire. It is noted that no additional salts were put in aqueous. (D) Amperometric  $i-t$  curve of collisions of the toluene emulsion droplets (5 mM rubrene + 400 mM IL-PA) in 3.35 pM located in 5 mM TBAClO<sub>4</sub> aqueous on the Pt UME biased at 0.9 V vs. Ag wire. (E) Amperometric  $i-t$  curve of collisions of the toluene emulsion droplets (5 mM rubrene + 400 mM IL-PA) in 5 mM NaTPB aqueous on the Pt UME biased at 0.9 V vs. Ag wire.

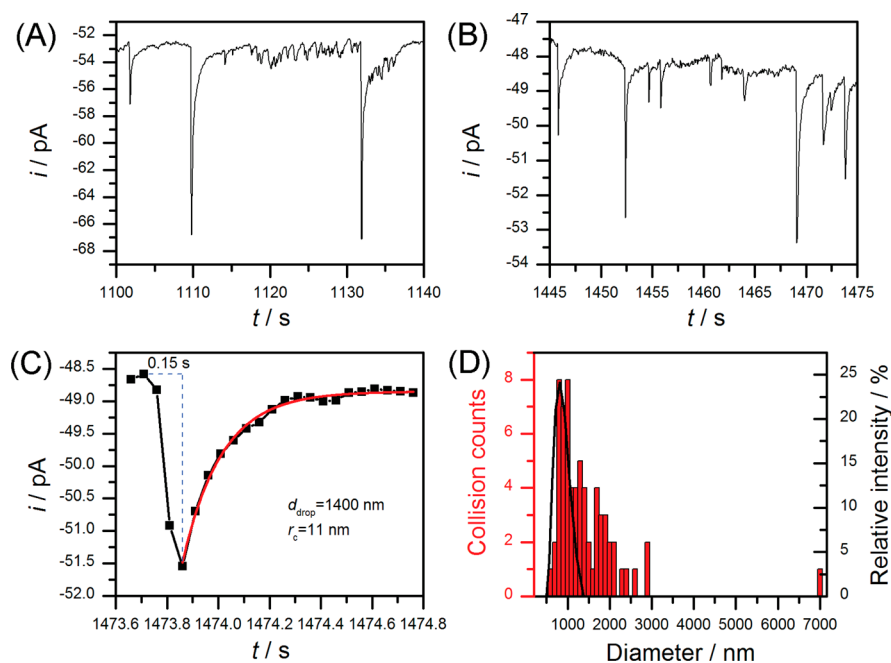


**Figure 4.** (A, B) Zoom-in ranges of 1100–1140 s and 1445–1475 s of Figure 3B, respectively. (C) Zoom-in  $i$ - $t$  curve of a single current spike between 1473.6 and 1474.8 s. The experimental data were sampled every 50 ms (black squares). The fitted  $i$ - $t$  curve (red line) was obtained using eq S16 and by performing regression analysis with an exponential decay model. The  $d_{\text{drop}}$  and  $r_c$  are calculated from the integrated charge and eqs S13 and S16, respectively. (D) Comparison of the emulsion droplets size distribution obtained from eq S13 (red bars) and that from DLS measurement (black line).

different scenarios to facilitate the electron transfer: (1) the product cation will leave the oil droplet, (2) a cation that is soluble in the oil phase will leave the oil droplet and enter the aqueous phase, or (3) an anion in the aqueous phase will enter the oil droplet. The concentration of ionic species initially in the aqueous phase is low ( $\geq 18.2 \text{ M}\Omega \text{ cm}$ ). The addition of ions from the emulsion is negligible considering the hydrophobicity of the toluene, rubrene, and ionic liquid (IL-PA) that make up the emulsion system. Even though there is a small amount of ions in the aqueous phase, that is, from water autodissociation, the hydrophilic nature of these ions would require a very high ion transfer potential that is outside the potential window of this system.<sup>2</sup> To confirm this, we observed that there were no current spikes during the collision experiment conducted using the same toluene droplets in 5 mM NaOH aqueous continuous phase (red line, Figure 3A). This is because  $\text{OH}^-$  is an extremely hydrophilic anion<sup>25</sup> that is not able to cross the ITIES to facilitate electron transfer in the obtainable potential window.

Clear current spikes are observed in Figure 3B–E with  $\text{TBA}^+$  or  $\text{THA}^+$  inside the toluene droplet; or  $\text{ClO}_4^-$  or  $\text{TPB}^-$  in the aqueous phase. This implies that transfer of other ions, rather than  $\text{R}^{\bullet+}$  or cation of IL-PA, across the o/w boundary, enables electrolysis of rubrene. The average current magnitude of spikes in the presence of  $\text{TBA}^+$ ,  $\text{THA}^+$ , or  $\text{ClO}_4^-$  transfer was similar. The zeta potential of the emulsion (stabilized by IL-PA) measured by DLS is negative, implying that the overall charge of the emulsion droplet is negative.<sup>17,20</sup> Because the overall charge is negative, the stability of the emulsion system is susceptible to small, positively charged ions, which explains why NaTPB, a polar salt composed of a hydrophilic and a hydrophobic ion,<sup>26</sup> causes the emulsion droplets to aggregate. This effect is shown in Figure S2C, which displays a cloudy and unstable emulsion compared to an emulsion system without

this sodium salt in water (Figure S2B). Thus, weakly coordinating cation salts can be used to avoid emulsion agglomeration and to see homogeneous blips during the collision measurements.

**TBA<sup>+</sup> Transfer from Oil Phase.** The diffusional flux of emulsion droplets to the electrode surface can be understood in a stochastic sense by considering the frequency with which droplets collide with the UME surface (eq S12). The diffusion coefficient of an 894 nm diameter emulsion droplet, calculated via the Stokes–Einstein relationship (eq S11), is  $5.49 \times 10^{-9} \text{ cm}^2 \text{ s}^{-1}$ . By means of eq S12, the predicted collision frequency of emulsion droplets by diffusion is 0.02 Hz. The experimentally observed frequency is  $0.03 \pm 0.01 \text{ Hz}$  based on three experimental replicates (0.05 Hz for Figure 3B), which matches well with the predicted value. Figure 4A and B show the zoom-in ranges of 1100–1140 s and 1445–1475 s of Figure 3B, respectively. The successful observation of Faradaic current (spikes in  $i$ - $t$  curve) implies that  $\text{TBA}^+$  enters into the water phase from the toluene droplet phase and facilitates the electrolysis of rubrene. The current decays exponentially with time, which is similar to the bulk electrolysis model employed in our prior research.<sup>17,19,20</sup> Because ion transfer across the o/w interface is a fast and reversible process,<sup>27</sup> it will not complicate the bulk electrolysis model employed in this study assuming both the droplet volume (calculated from  $d_{\text{drop}}$  in eq S13) and the contact radius  $r_c$  remain constant. In our model, the droplet adsorbs to the UME, and electrolysis is carried out at a small contact area, causing the initial current spike. The current then decays exponentially with time. Figure 4C gives a quantitative analysis of a 1400 nm droplet collision using eq S16 and the theoretical curve from bulk electrolysis theory (red line) agrees well with the experimental data (black squares). The contact radius  $r_c$  (11 nm) was obtained from the best fit using the bulk electrolysis model. Figure 4D demonstrates the moderate

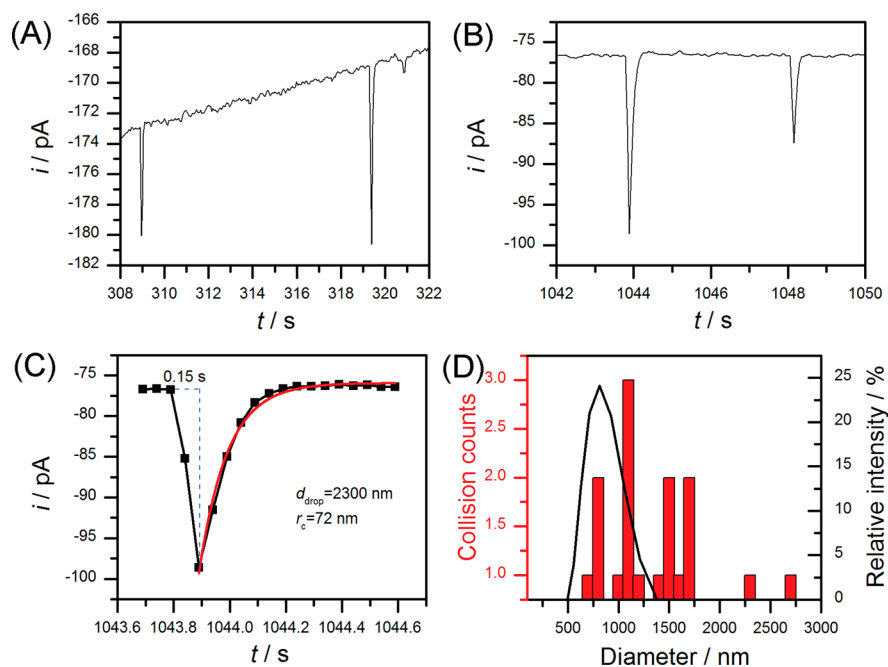


**Figure 5.** (A, B) Zoom-in ranges of 308–322 and 1042–1050 s of Figure 3D, respectively. (C) Zoom-in  $i$ – $t$  curve of a single current spike between 1043.6 and 1044.6 s. The experimental data were sampled every 50 ms (black squares). The fitted  $i$ – $t$  curve (red line) was obtained using eq SI6 and by performing regression analysis with an exponential decay model. The  $d_{\text{drop}}$  and  $r_c$  are calculated from the integrated charge and eqs SI3 and SI6, respectively. (D) Comparison of the emulsion droplets size distribution obtained from eq SI3 (red bars) and that from DLS measurement (black line).

agreement between the emulsion size distribution based on the electrochemical results (eq SI3) and the DLS result. Furthermore, the electrochemical method detected big droplets (1500–7000 nm) that were not detected and reported via the DLS measurement.

**$\text{ClO}_4^-$  Transfer from Aqueous Phase.** For three experimental replicates of collisions of the 3.35 pM of toluene emulsion droplets (5 mM rubrene + 400 mM IL-PA) in 5 mM  $\text{TBAClO}_4$  aqueous (0.011 Hz for Figure 3D) the experimentally observed frequency was  $0.014 \pm 0.005$  Hz, which is comparable to the theoretical value (0.02 Hz). Figure 5A,B show the zoom-in ranges of 308–322 and 1042–1050 s of Figure 3D, respectively. We used eq SI6 to obtain the best-fit  $i$ – $t$  curve (red line, Figure 5C) for the collision of a 2300 nm droplet and the theoretical value agrees well with the experimental data. A contact radius  $r_c$  (72 nm) was obtained from the best fit with eq SI6. With respect to the  $r_c$  value obtained in Figure 4C, it seems that a bigger emulsion droplet  $d_{\text{drop}}$  has a bigger contact radius with the UME. Furthermore,  $r_c$  and  $d_{\text{drop}}$  are correlated in an exponential increase style that has been found before.<sup>19,20</sup> The electrolysis current decays with time because the rubrene in the droplet becomes depleted (mass transfer inside the tiny droplet is very efficient) during the electrolysis. The successful observation of Faradaic current (spikes in  $i$ – $t$  curve) implies that  $\text{ClO}_4^-$  enters into the toluene droplet from the aqueous continuous phase and facilitates the electrolysis of rubrene. Displayed in Figure 5D (red bars), the emulsion droplet size distribution was obtained with eq SI3. The difference between the electrochemical data (1100 nm) and DLS values (average diameter of 894 nm) can be ascribed to the dramatic difference (charge transfer vs light scattering) in the operating principle of these two methods and the polydispersity of the IL-PA stabilized emulsion.

**Estimation of the Formal Ion Transfer Potential across the o/w Interface.** One interesting outcome of the electrochemical collision experiments is the estimation of the formal ion transfer potential across the toluene/water interface. Figure 6A shows the  $i$ – $t$  curves of the collision experiments of 3.35 pM of toluene emulsion droplets (5 mM rubrene + 5 mM TBAOTf + 400 mM IL-PA) in water (no additional ions). The average magnitude of the current spikes decreases with the decrease in the potential applied at the UME, implying that the relation of average current peak height versus potential can be used to estimate the formal ion transfer potential. Figure 6B shows the comparison between the built voltammogram from Figure 6A and that (rubrene CV in the bulk toluene phase) from Figure 2A. The built voltammogram, that is, the sampled-current voltammogram, was made by plotting the average peak current of blips recorded at different potential steps versus the potential to which the step takes place. For convenience, both voltammograms in Figure 6B were plotted in normalized current. Due to the energy required for the ion transfer at the o/w interface during the rubrene electrolysis confined in the toluene droplet, it is expected that the built voltammogram will have a half-wave potential ( $E_{1/2}$ ) more positive with respect to that recorded in the bulk oil phase. This effect has been corroborated and shown in Figure 6B. Due to water oxidation at more positive potentials, data points at these potentials are omitted from the sampled-current voltammogram (refer to the inset in Figure 2A). Because 0.9 V is sufficiently high to reach the foot of a well-defined sampled-current voltammogram,  $\sim 0.85$  V was designated as the estimated  $E_{1(1/2)}$  (refer to eq SI15) of the ET-IT process.  $E_{2(1/2)}$  is equal to 0.697 V obtained from Figure 2B. Invoking eq SI19, we can calculate an estimated formal ion transfer potential of  $\text{TBA}^+$  ( $\Delta_w \phi_{\text{TBA}^+}^{\circ}$ ) across the toluene/water interface using eq 3,

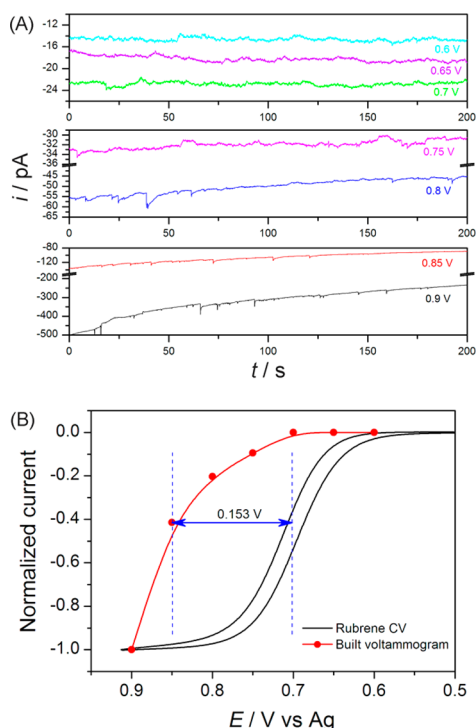


**Figure 6.** (A) Amperometric  $i-t$  curves of collisions of the toluene emulsion droplets (5 mM rubrene + 5 mM TBAOTf + 400 mM IL-PA) in 3.35 pM on the Pt UME biased from 0.9 to 0.6 V vs. Ag wire. It is noted that no additional salts were put in aqueous and data break was made for clearer comparison. (B) Comparison between the built voltammogram based on the average current magnitude of collision spikes at different potentials in (A) vs potential and the CV of rubrene in the bulk toluene phase with 400 mM IL-PA as supporting electrolyte.

$$\Delta_w \phi_{\text{TBA}^+}^{\circ'} = \Delta E_{1/2} - \frac{RT}{F} \ln \left( \frac{c_{\text{R}}^{\circ,0}}{c_{\text{TBA}^+}^{\circ}} \sqrt{\frac{D_{\text{R}}^{\circ}}{D_{\text{TBA}^+}^{\circ}}} \right) - E_{\text{ref1}}^{\circ} + E_{\text{ref2}}^{\circ} \quad (3)$$

in which  $\Delta E_{1/2} = 0.85 - 0.697 = 0.153$  V,  $D_{\text{R}}^{\circ}$  is  $2.21 \times 10^{-6} \text{ cm}^2 \text{ s}^{-1}$ ,  $D_{\text{TBA}^+}^{\circ}$  is  $7.35 \times 10^{-6} \text{ cm}^2 \text{ s}^{-1}$  reported before,<sup>28</sup>  $c_{\text{R}}^{\circ,0} = c_{\text{TBA}^+}^{\circ}$ ,  $E_{\text{ref1}}^{\circ} = 0.358$  V + SHE, and  $E_{\text{ref2}}^{\circ} = 0.944$  V + SHE, SHE represents standard hydrogen electrode in water.  $E_{\text{ref1}}^{\circ}$  is evaluated based on the half-wave potential of 1 mM FcMeOH at  $10 \mu\text{m}$  Pt UME vs. a Ag wire (0.084 V in Figure S3) and the reported value,<sup>29</sup> 0.2 V versus SCE (saturated calomel electrode, 0.242 V vs SHE).  $E_{\text{ref2}}^{\circ}$  is evaluated based on  $E_{2(1/2)}$  of 0.697 V vs a Ag wire and the estimated value of formal redox potential of rubrene in toluene with respect to aqueous SHE of 1.641 V (Figure S4 and eq SI31).

Finally, the formal ion transfer potential of  $\text{TBA}^+$ ,  $\Delta_w \phi_{\text{TBA}^+}^{\circ'}$ , is calculated to be 0.754 V in the inner potential scale. This estimated value is much higher than those obtained at the DCE/w (0.230 V) and NB/w (0.248 V) interfaces.<sup>30</sup> Nonetheless, this dramatic difference can be reconciled considering the significant difference in the dielectric constants of these three solvents and the classical electrostatic solvation model of Born (eq SI29). The formal Gibbs transfer energy of  $\text{TBA}^+$  from toluene to water phase is calculated via the following equation:  $\Delta G_{\text{tr,TBA}^+}^{\circ',\text{o}\rightarrow\text{w}} = F \Delta_w \phi_{\text{TBA}^+}^{\circ'} = 72.8 \text{ kJ mol}^{-1}$ .<sup>5</sup>

**Collision Experiments of the Toluene (DMFc/DEC + IL-PA)/Water Emulsion Droplets.** In addition to rubrene, other hydrophobic redox probes including DMFc and DEC (Figure S5) were also tested in EDR experiments. Contrary to the rubrene experiment, current spikes could be observed without the addition of ions in either the oil or water phase, which implies that the cation radicals are soluble in the aqueous phase in the electric field even though DMFc and DEC contain hydrophobic substituents. Figure 7A,B displays the  $i-t$  curves of the collision experiments of 25 pM toluene emulsion

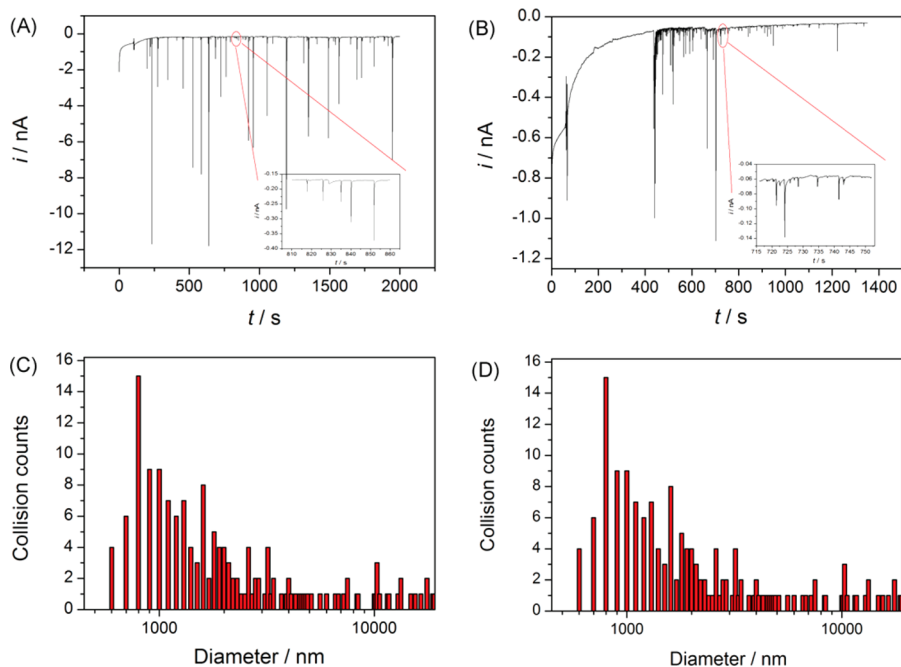


**Figure 7.** (A, B) Amperometric  $i-t$  curves of collisions of the toluene emulsion droplets (20 mM DMFc + 400 mM IL-PA, (A); 20 mM DMFc + 20 mM TBAOTf + 400 mM IL-PA, (B)) in 25 pM on the  $25 \mu\text{m}$  Pt UME and  $10 \mu\text{m}$  Pt UME biased at 0.8 V vs Ag wire, respectively. Note that no additional salts were put in aqueous. (C) and (D) The corresponding emulsion droplets size distribution for (A) and (B) calculated by eq SI3.

droplets (20 mM DMFc + 400 mM IL-PA for Figure 7A, 20 mM DMFc + 20 mM TBAOTf + 400 mM IL-PA for Figure 7B) in water (no additional ions). Figure 7C and D show the corresponding emulsion size distributions for the cases of Figure 7A and B, respectively, which show that the droplets are about a micrometer. This value is close to the toluene (rubrene)/water emulsions.

## CONCLUSIONS

In this work, we have found that rubrene, an extremely hydrophobic molecule, can be employed as a redox probe trapped in femtoliter toluene emulsion droplets to observe electron transfer coupled ion transfer processes during single emulsion droplet collision electrochemical measurements. Other hydrophobic redox probes, DMFc and DEC, were also tested, but the charge neutrality in the oil phase is maintained by expulsion of oxidized redox probe rather than the ionic flux of other ions across the o/w boundary. Collision frequency, emulsion size distribution,  $i-t$  behavior of collision spikes, and formal ion transfer potentials were analyzed based on the theory developed in this work and with rubrene as the redox probe. Rubrene oxidation in the toluene emulsion droplet follows the bulk electrolysis model with the help from the simultaneous/fast ion (cation or anion) transfer through the o/w barrier. The bulk electrolysis can be achieved within seconds in these femtoliter reactors, which extends the earlier works.<sup>17,19,20</sup> This work lays the foundation for the electrochemistry at the ITIES with nonpolar solvents as the organic phases (forming interfaces with water), which cannot be addressed easily via other methods and will benefit quantitative analysis of electrochemistry in solvents with extremely low dielectric constants featured with a broader potential window. Employing monodispersed emulsions and a well-defined reference electrode applicable in both water and oil phases will spur this methodology to solve a wider range of electrochemical problems. The method also provides access to the true heterogeneous bimolecular electron transfer rate at the ITIES uncoupled from ion transfer rate. This requires an extremely lipophilic redox species like rubrene found herein to be maintained within the oil phase during the electronic communication with the hydrophilic redox species like ferricyanide in the aqueous phase.<sup>31</sup>

## ASSOCIATED CONTENT

### Supporting Information

The Supporting Information is available free of charge on the ACS Publications website at DOI: 10.1021/acs.analchem.6b01747.

Supporting figures and tables, as well as additional computational details (PDF).

## AUTHOR INFORMATION

### Corresponding Author

\*E-mail: ajbard@mail.utexas.edu.

### Author Contributions

†These authors contributed equally to this work (H.D. and J.E.D.).

### Notes

The authors declare no competing financial interest.

## ACKNOWLEDGMENTS

We gratefully acknowledge the financial support from the National Science Foundation (Grants CHE-1405248 to A.J.B. and CHE-1346572 to S.H.S.) and the Welch Foundation (Grant No. F-0021). J.E.D. acknowledges the National Science Foundation Graduate Research Fellowship (Grant No. DGE-1110007). H.D. thanks the helpful discussions and help from Dr./Prof. Yan Li (Northwest University, Xi'an, China), Dr. Nataraju Bodappa, Dr. Xiaole Chen, Dr. Hsien-Yi Hsu, and Dr. Pekka Peljo (LEPA, EPFL, Switzerland) for this work. S.K. acknowledges the support of the German Federal Ministry of Education and Research (BMBF-Bundesministerium für Bildung und Forschung, Grant No. 031A123 to S.K.). The authors also acknowledge Dr. Lauren M. Strawsine for helpful editing.

## REFERENCES

- (1) CRC Handbook of Chemistry and Physics, 85th ed.; Lide, D. R., Ed.; CRC Press: Boca Raton, FL, 2005.
- (2) Atkins, P. W. *Physical Chemistry*, 4th ed.; Oxford University Press: Oxford, 1990.
- (3) Girault, H. H. In *Electroanalytical Chemistry*; Bard, A. J., Zoski, C. G., Eds., CRC Press, 2010; Vol. 23; pp 1–104.
- (4) Samec, Z.; Mareček, V.; Koryta, J.; Khalil, M. W. *J. Electroanal. Chem. Interfacial Electrochem.* **1977**, *83*, 393–397.
- (5) Deng, H.; Peljo, P.; Cortés-Salazar, F.; Ge, P.; Kontturi, K.; Girault, H. H. *J. Electroanal. Chem.* **2012**, *681*, 16–23.
- (6) Deng, H.; Stockmann, T. J.; Peljo, P.; Opallo, M.; Girault, H. H. *J. Electroanal. Chem.* **2014**, *731*, 28–35.
- (7) Shi, C.; Anson, F. C. *Anal. Chem.* **1998**, *70*, 3114–3118.
- (8) Quentel, F.; Mirčeski, V.; L'Her, M. *Anal. Chem.* **2005**, *77*, 1940–1949.
- (9) Deng, H.; Huang, X.; Wang, L.; Tang, A. *Electrochem. Commun.* **2009**, *11*, 1333–1336.
- (10) Deng, H.; Huang, X.; Wang, L. *Langmuir* **2010**, *26*, 19209–19216.
- (11) Taylor, G.; Girault, H. H. *J. Electroanal. Chem. Interfacial Electrochem.* **1986**, *208*, 179–183.
- (12) Deng, H.; Peljo, P.; Momotenko, D.; Cortés-Salazar, F.; Jane Stockmann, T.; Kontturi, K.; Opallo, M.; Girault, H. H. *J. Electroanal. Chem.* **2014**, *732*, 101–109.
- (13) Sun, P.; Zhang, Z.; Gao, Z.; Shao, Y. *Angew. Chem., Int. Ed.* **2002**, *41*, 3445–3448.
- (14) Moumouzias, G.; Ritzoulis, G. *J. Chem. Eng. Data* **1997**, *42*, 710–713.
- (15) Shul, G.; Adamiak, W.; Opallo, M. *Electrochem. Commun.* **2008**, *10*, 1201–1204.
- (16) Bond, A. M.; Mann, T. F. *Electrochim. Acta* **1987**, *32*, 863–870.
- (17) Kim, B.-K.; Boika, A.; Kim, J.; Dick, J. E.; Bard, A. J. *J. Am. Chem. Soc.* **2014**, *136*, 4849–4852.
- (18) Dick, J. E.; Renault, C.; Kim, B.-K.; Bard, A. J. *Angew. Chem., Int. Ed.* **2014**, *53*, 11859–11862.
- (19) Kim, B.-K.; Kim, J.; Bard, A. J. *J. Am. Chem. Soc.* **2015**, *137*, 2343–2349.
- (20) Li, Y.; Deng, H.; Dick, J. E.; Bard, A. J. *Anal. Chem.* **2015**, *87*, 11013–11021.
- (21) Caamaño, S. *Ph.D. dissertation*, Colorado State University, 2010.
- (22) Fan, F. F.; Fernandez, J.; Liu, B.; Mauzeroll, J.; Zoski, C. G. In *Handbook of Electrochemistry*; Zoski, C. G., Ed.; Elsevier: Amsterdam, 2007; pp 189–199.
- (23) Bowen, E. J.; Steadman, F. *J. Chem. Soc.* **1934**, 1098–1101.
- (24) Bard, A. J.; Faulkner, L. R. *Electrochemical Methods*; 2nd ed.; John Wiley & Sons: New York, 2001.
- (25) Zhou, M.; Gan, S.; Zhong, L.; Su, B.; Niu, L. *Anal. Chem.* **2010**, *82*, 7857–7860.
- (26) Johans, C.; Behrens, M. A.; Bergquist, K. E.; Olsson, U.; Manzanara, J. A. *Langmuir* **2013**, *29*, 15738–15746.

(27) Li, Q.; Xie, S.; Liang, Z.; Meng, X.; Liu, S.; Girault, H. H.; Shao, Y. *Angew. Chem., Int. Ed.* **2009**, *48*, 8010–8013.

(28) Kim, H.; Revzin, A.; Gosting, L. J. *J. Phys. Chem.* **1973**, *77*, 2567–2570.

(29) Jimenez, A. I. P.; Challier, L.; Di Pisa, M.; Guille-Collignon, M.; Lemaitre, F.; Lavielle, S.; Mansuy, C.; Amatore, C.; Labbé, E.; Buriez, O. *Electrochem. Commun.* **2015**, *54*, 41–45.

(30) Shao, Y. In *Handbook of Electrochemistry*; Zoski, C. G., Ed.; Elsevier: Amsterdam, 2007; pp 785–809.

(31) Osakai, T.; Ichikawa, S.; Hotta, H.; Nagatani, H. *Anal. Sci.* **2004**, *20*, 1567–1573.